Quasi-3D Finite-Element Method for Simulating Cylindrical Induction Heating Devices

Laura A. M. D'Angelo[1,2], Herbert De Gersem[1,2]
[1]Graduate School of Computational Engineering, TU Darmstadt, Germany, degersem@temf.tu-darmstadt.de
[2]Institut für Theorie Elektromagnetischer Felder (TEMF), TU Darmstadt, Germany

The 3D magnetic-field and temperature distibutions in a cylindrically symmetic induction-heating device are simulated with a quasi-3D finite-element (FE) method using tensor-product shape functions, combining standard polynomial FEs defined at a 2D triangulation with harmonic functions along the azimuthal direction.

***Index Terms*—Eddy currents, Finite element analysis, Induction heating, Multiphysics.**

I. Introduction

STANDARD 2D axisymmetric finite-element (FE) simulation is not applicable in case of a cylindrically symmetric geometry combined with an asymmetric excitation or boundary condition [1], [2], [3]. The change to a standard 3D FE model comes together with a considerable increase in computation cost [4]. In this paper, a *quasi-3D* FE method is developed for a coupled magnetoquasistatic-thermal problem and illustrated for a cylindrical induction-heating example [5].

II. Axisymmetric Multiphysics FE Model

The magnetoquasistatic and thermal formulations discretized by the edge FE shape functions $\vec{w}_j(r,z)$ and nodal FE shape functions $N_j(r,z)$ [6](Fig. 1) read

$$\mathbf{K}_\nu \widehat{\mathbf{a}} + \jmath\omega\mathbf{M}_\sigma \widehat{\mathbf{a}} = \widehat{\widehat{\mathbf{j}}}_{\mathrm{s}} \quad ; \tag{1}$$

$$\mathbf{K}_\lambda \mathbf{u} + \mathbf{M}_c \frac{\mathrm{d}\mathbf{u}}{\mathrm{d}t} + \mathbf{R}_h \mathbf{u} = \mathbf{R}_h \mathbf{u}_{\text{fluid}} + \mathbf{q}_{\mathrm{v}} \quad , \tag{2}$$

where (r,φ,z) is a cylindrical coordinate system, $\widehat{\mathbf{a}}$ and $\mathbf{u}$ collect the degrees of freedom (DoFs) for the magnetic vector potential and the temperature respectively, $\mathbf{u}_{\text{fluid}}$, $\widehat{\widehat{\mathbf{j}}}_{\mathrm{s}}$ and $\mathbf{q}_{\mathrm{v}}$ contain the ambient temperatures, electric currents and heat losses respectively, and $\mathbf{K}_\nu$, $\mathbf{M}_\sigma$, $\mathbf{K}_\lambda$, $\mathbf{M}_c$ and $\mathbf{R}_h$ denote the FE reluctance, electric conductance, thermal conductance, thermal heat-capacitance and boundary-convection matrices respectively [7], [8], [9].

III. Quasi-3D Multiphysics FE Model

The azimuthal asymmetry of the temperature distribution

$$T(r,\varphi,z) = \sum_{q\in\Lambda}\sum_{j} \mathrm{Re}\{\underline{u}_{j,q} \underbrace{N_j(r,\varphi,z)(r,z)e^{+\jmath q\varphi}}_{\underline{W}_{j,q}(r,\varphi,z)}\} \tag{3}$$

is resolved by tensor-product FE shape functions $\underline{W}_{j,q}(r,\varphi,z)$ combining the standard nodal FEs $N_j(r,z)$ defined at a 2D cross-sectional mesh with harmonic functions $e^{+\jmath q\varphi}$ [10], [11], [12]. Hereby, Λ is a well-chosen set of harmonic functions and $\underline{u}_{j,q}$ gathers the DoFs. The Ritz-Galerkin procedure carried out

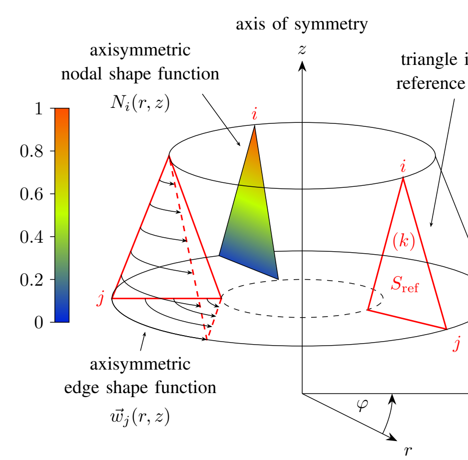

Fig. 1. Edge FE shape function $\vec{w}_j(r,z)$ and nodal FE shape function $N_i(r,z)$ for resolving the cylindrically symmetric magnetic vector potential and temperature at a 2D triangulation of the (r,z)-plane. The z-axis is the axis of symmetry.

with the test functions $\underline{W}^*_{i,p}(r,\varphi,z) = N_i(r,z)e^{-\jmath p\varphi}$, $\forall p\in\Lambda$ leads to the discrete 3D thermal submodel

$$\underline{\mathbf{M}}_c \frac{\mathrm{d}\underline{\mathbf{u}}}{\mathrm{d}t} + \underline{\mathbf{K}}_\lambda \underline{\mathbf{u}} + \underline{\mathbf{R}}_h \underline{\mathbf{u}} = \underline{\mathbf{q}}_{\mathrm{v}} + \underline{\mathbf{R}}_h \underline{\mathbf{u}}_{\text{fluid}} \tag{4}$$

where the stiffness, mass and convection matrices are

$$\underline{\mathbf{K}}_\lambda = \mathbf{I}\otimes\mathbf{K}_\lambda + \mathbf{P}\otimes\mathbf{N}_\lambda \quad ; \tag{5}$$

$$\underline{\mathbf{M}}_c = \mathbf{I}\otimes\mathbf{M}_c \quad ; \tag{6}$$

$$\underline{\mathbf{R}}_h = \mathbf{I}\otimes\mathbf{R}_h \quad , \tag{7}$$

and where $\otimes$ denotes the Kronecker product, $\mathbf{I}\in\mathbb{R}^{|\Lambda|\times|\Lambda|}$ is the identity matrix, $\mathbf{K}_\lambda$, $\mathbf{M}_c$ and $\mathbf{R}_h$ are the 2D axisymmetric FE stiffness, mass and convection matrices, $\mathbf{P} = \mathrm{diag}\left(m_1^2,\ldots,m_{|\Lambda|}^2\right)$ contains the squared harmonic orders at its diagonal and $\mathbf{N}_\lambda$ is a mass-like matrix with entries $\mathbf{N}_{\lambda,ij} = \int_V \lambda N_i N_j \,\mathrm{d}V$ assembled for the thermal conductivity λ at the 2D cross-sectional mesh. The treatment of the magnetoquasistatic subproblem is analogous.

The quasi-3D FE technique allows to consider cylindrically asymmetric thermal convection, which gives rise to an asym-

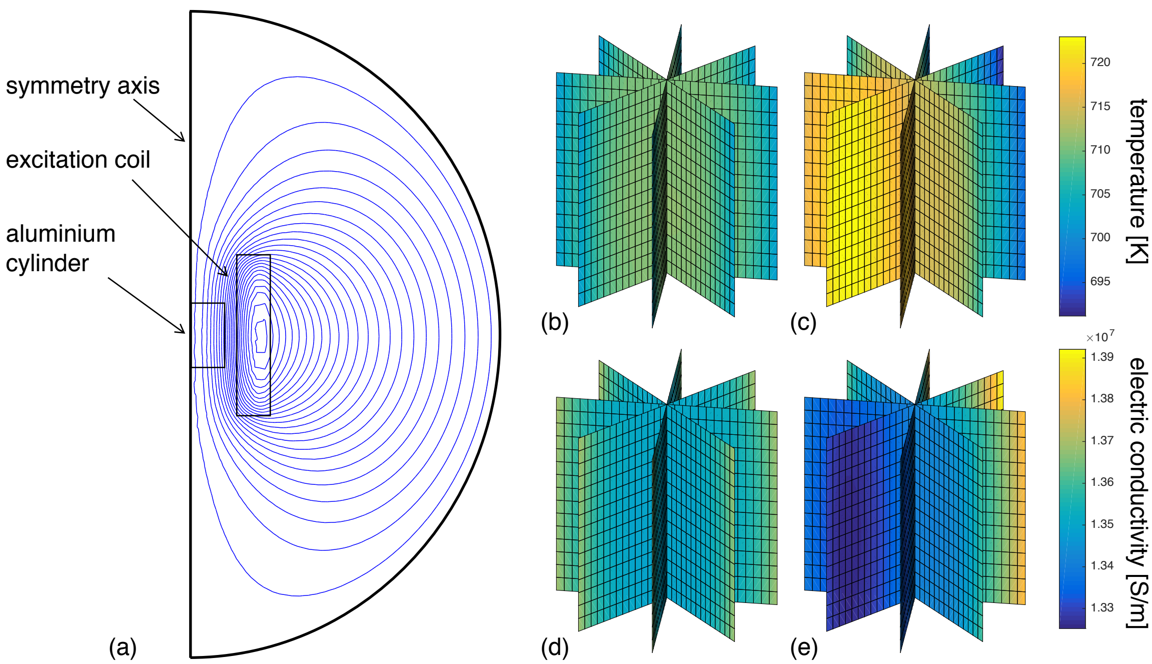

Fig. 2. Cylinder heated by induction: (a) geometry and magnetic flux lines; (b) and (c): temperature distribution; (d) and (e): distribution of the electric conductivity. Parts (b) and (d) show the situation with cylindrical symmetry. Parts (c) and (e) show the asymmetric situation.

metric temperature distribution and, alongside the temperature-dependent electric conductivity, an asymmetric current distribution. Further azimuthal asymmetries may originate from the combination of asymmetric field distributions and nonlinear conductivities. The method is extensively validated for benchmarks for which analytical solutions exist. The convergence study indicates an exponential convergence with respect to the number of considered harmonics and a polynomial convergence with respect to the number of 2D mesh nodes, which confirms theoretical considerations.

IV. Example and Conclusions

The magnetically-thermally coupled quasi-3D FE method is applied to an aluminum cylinder submitted to the magnetic field excited by a cylindrical coil and cooled by thermal convection (Fig. 2a). Figs 2b-e show cross-sections of the cylinder at 8 azimuthal positions. In case of a cylindrically symmetric air cooling, the heat transfer by convection and consequently also the magnetic-field and temperature distributions are cylindrically symmetric, which is observed in Fig. 2b and Fig. 2d by the identical color distributions in all cross-sections. In case of an air flow from one side (from the back side in Fig. 2), the cylindrical symmetry is lost. The quasi-3D FE calculations still make use of the same 2D mesh. The temperature is represented by 4 azimuthally harmonic field components, whereas 1 additional azimuthal harmonic is considered for the electric scalar potential. The temperature distribution shown in Fig. 2c clearly indicates the better cooling at the back side. The electric conductivity shown in Fig. 2d spans a larger range than for the axisymmetric case. From the figures, it is obvious that the asymmetric cooling at the cylinder hull changes the field distributions drastically. Hence, a full 3D field simulation is mandatory. The computationally cheap quasi-3D FE approach proposed here is capable of calculating the 3D field distributions.

References

[1] G. Bedrosian, M. V. K. Chari, M. Shah, and G. Theodossiou, “Axiperiodic finite element analysis of generator end regions - Part I - Theory,” *IEEETransMagn*, vol. 25, no. 4, pp. 3067–3069, jul 1989.

[2] S. Kurz, B. Auchmann, and B. Flemisch, “Dimensional reduction of field problems in a differential-forms framework,” *COMPEL*, vol. 28, no. 4, pp. 907–921, 2009.

[3] P. Raumonen, S. Suuriniemi, and L. Kettunen, “Dimensional reduction of electromagnetic boundary value problems,” *Bound. Value Probl.*, no. 9, Jul. 2011.

[4] P. Karban, F. Mach, I. Dolezel, and J. Barglik, “Higher-order finite element modeling of rotational induction heating of nonferromagnetic cylindrical billets,” *COMPEL*, vol. 30, no. 5, pp. 1517–1527, 2011.

[5] S. Lupi, M. Forzan, and A. Aliferov, *Induction and Direct Resistance Heating*. Springer, 2015.

[6] F. Henrotte, B. Meys, H. Hedia, P. Dular, and W. Legros, “Finite element modelling with transformation techniques,” *IEEE Trans. Magn.*, vol. 35, no. 3, pp. 1434–1437, May 1999.

[7] O. Bíró and K. Preis, “On the use of the magnetic vector potential in the finite-element analysis of three-dimensional eddy currents,” *IEEE Trans. Magn.*, vol. 25, no. 4, pp. 3145–3159, Jul. 1989.

[8] M. Clemens, E. Gjonaj, P. Pinder, and T. Weiland, “Self-consistent simulations of transient heating effects in electrical devices using the Finite Integration Technique,” *IEEE Trans. Magn.*, vol. 37, no. 5, pp. 3375–3379, Sep. 2001.

[9] J. Driesen, R. J. M. Belmans, and K. Hameyer, “Computation algorithms for efficient coupled electromagnetic-thermal device simulation,” *IEE. Proc. Sci. Meas. Tech.*, vol. 149, no. 2, pp. 67–72, Mar. 2002.

[10] S. Koch, H. De Gersem, and T. Weiland, “Hybrid finite-element method for discretising cylindrically symmetric parts in electrotechnical models,” *IET. Sci. Meas. Tech.*, vol. 1, no. 1, pp. 6–11, Jan. 2007.

[11] P. Bettini and R. Specogna, “A novel approach for solving three dimensional eddy currentproblems in fusion devices,” *Fusion Engineering and Design*, vol. 96-97, pp. 703–706, 2015.

[12] D. Doornaert, C. Glorieux, H. De Gersem, R. Puers, W. Spileers, and J. Blanckaert, “Quasi-3-D finite-element method for cylindrically symmetric models with small eccentricities,” *IEEE Trans. Magn.*, vol. 52, no. 3, p. 7401404, Mar. 2016.